Research Square

Preprints are preliminary reports that have not undergone peer review.
They should not be considered conclusive, used to inform clinical practice,
or referenced by the media as validated information.

Early Thyroid Injury and Parathyroid Resistance Following Ionizing Radiation: Evidence of Paradoxical Hsp-90 Downregulation

Şeyda Belli

seyda.belli@sbu.edu.tr

Health Sciences University

İsmail Safa Poyrazoğlu

Health Sciences University

Eren Altun

Health Sciences University

Nida Sünnetçi Arkan

Health Sciences University

Research Article

Keywords: Cellular stress response, Endocrine radiosensitivity, HSP-90, Ionizing radiation, Parathyroid gland, Thyroid gland

Posted Date: April 11th, 2026

DOI: https://doi.org/10.21203/rs.3.rs-9328347/v1

License: This work is licensed under a Creative Commons Attribution 4.0 International License.
Read Full License

Additional Declarations: No competing interests reported.

Version of Record: A version of this preprint was published at Journal of Molecular Histology on September 18th, 2026. See the published version at https://doi.org/10.1007/s10735-026-10975-0.

Abstract

Objective

Ionizing radiation (IR) is widely used in the treatment of head and neck malignancies; however, its early effects on adjacent endocrine tissues remain insufficiently characterized. This study aimed to investigate early post-irradiation structural and molecular alterations in the thyroid and parathyroid glands, with a particular focus on HSP-90-mediated proteostasis.

Materials and Methods

Male Wistar-Hannover rats were assigned to control or irradiation groups and exposed to a single 18 Gy dose of IR to the head and neck region. On day 21, thyroid and parathyroid tissues were evaluated histopathologically and immunohistochemically for morphological changes and HSP-90 expression.

Results

Irradiated thyroid tissue exhibited significant vascular congestion ($p = 0.031$), inflammatory infiltration ($p = 0.040$), and epithelial desquamation ($p = 0.006$). Notably, HSP-90 expression in thyroid follicular cells demonstrated a **paradoxical downregulation**, being significantly reduced compared with controls ($p = 0.011$). In contrast, parathyroid glands showed preserved architecture and stable HSP-90 expression ($p = 0.914$).

Conclusion

A single high-dose IR exposure induces early microstructural injury in the thyroid while paradoxically suppressing HSP-90-mediated stress responses, whereas the parathyroid gland appears relatively resistant at this stage. These findings highlight organ-specific differences in endocrine radiosensitivity and suggest that early impairment of proteostasis may contribute to radiation-induced thyroid vulnerability.

Introduction

Radiation can be broadly divided into ionizing radiation (IR) and non-ionizing radiation (non-IR) [1, 2]. IR includes photon radiation such as X-rays and γ-rays and particle radiation including electrons, protons, neutrons, carbon ions, and α- and β-particles [1–3]. By definition, IR carries sufficient energy to remove electrons from atoms or molecules, thereby ionizing them [1–3]. Non-IR comprises ultraviolet (UV) radiation, visible light, lasers, infrared, microwaves and radiofrequency waves, which generally lack the energy required to induce direct ionization [4, 5].

IR is widely used in medical diagnostics and therapy and provides substantial clinical benefit [6, 7]. Radiotherapy, predominantly employing X-rays and γ-rays, is a cornerstone treatment modality in head and neck cancers [6–9]. However, beyond its antitumor efficacy, IR can induce clinically relevant damage in normal tissues within the radiation field, including endocrine organs such as the thyroid and parathyroid glands [8–10].

Although the thyroid gland has classically been regarded as relatively resistant to acute radiation effects, it is particularly vulnerable to long-term sequelae of radiation exposure [10–13]. The hypothalamic-pituitary-thyroid axis is highly radiosensitive, and the degree of damage is influenced by radiation field, total dose and fractionation [10, 12]. Epidemiological data from atomic bomb survivors and nuclear accidents (Hiroshima, Nagasaki, Chernobyl) and from patients receiving therapeutic irradiation clearly demonstrate increased risks of hypothyroidism, nodular thyroid disease and thyroid carcinoma, especially when exposure occurs during childhood and adolescence [2, 10–13].

The thyroid gland is composed of thousands of follicles lined by follicular cells surrounding a thyroglobulin-rich colloid [12, 14]. Follicular thyrocytes actively transport iodide, synthesize thyroglobulin and produce thyroid hormones T3 and T4, processes that require high levels of protein synthesis and robust endoplasmic reticulum and mitochondrial function [12, 14]. Consequently, these cells are particularly susceptible to stressors such as heat, oxidative damage and radiation [14, 15].

Parathyroid glands also exhibit considerable metabolic activity and secrete parathyroid hormone but differ structurally from the thyroid, as chief cells are arranged in solid cords rather than forming follicles. Both thyroid and parathyroid tissues utilize heat shock proteins (HSPs), including HSP-70 and HSP-90, as part of the cellular stress response [15, 16]. Due to their high metabolic demand, parathyroid cells share core stress pathways with thyroid follicular cells; however, the absence of a follicular architecture implies that radiation-induced damage may manifest preferentially as alterations of the plasma membrane, subcellular organization and perinuclear compartments rather than follicular collapse [16]. These architectural and metabolic differences may underlie organ-specific radiosensitivity.

HSP-90 is a ubiquitously expressed molecular chaperone essential for multiple physiological processes, including cell cycle regulation, proliferation and hormone signaling [17, 18]. It assists in protein folding, stabilizes client proteins and facilitates repair or proteasomal degradation of misfolded proteins, thereby maintaining intracellular proteostasis [17–19]. Under stress conditions such as hyperthermia, oxidative stress or irradiation, HSP-90 levels are typically upregulated [18–20]. In the endocrine system, HSP-90 stabilizes thyroid hormone receptors (particularly TRβ) and various kinases and interacts with multiple nuclear receptors, including glucocorticoid, estrogen and thyroid hormone receptors [18, 19, 24].

In the immediate aftermath of IR exposure, cells experience DNA double-strand breaks, mitochondrial dysfunction, ATP depletion and a surge in reactive oxygen species (ROS) [20]. These events are accompanied by suppression of ribosomal RNA synthesis and a global inhibition of protein synthesis [20, 21]. Cells may transiently enter an energy-saving state in which even protective chaperone synthesis is attenuated [20, 21]. In highly active thyroid follicular cells, this can coincide with reduced thyroid

peroxidase synthesis, cessation of hormone production and a shift toward a quiescent state [14, 21]. During this early period, a transient decline in HSP-90 may occur before later adaptive upregulation [20, 21]. Thus, early post-irradiation dynamics of HSP-90 in the thyroid might reflect a failure or delay in mounting an adequate stress response.

Existing evidence on HSP-90 behavior in irradiated thyroid tissue is limited and partially contradictory. Some data indicate upregulation of HSP-90 under chronic or subchronic exposure, whereas decreased HSP-90 expression has been reported following non-ionizing radiation in rats [16, 23]. Furthermore, the parathyroid response to radiation, both morphologically and at the level of stress proteins, remains poorly characterized [11, 16].

In this context, the present study aimed to investigate the early post-irradiation (day 21) effects of a single high-dose IR exposure on thyroid follicular morphology and HSP-90 expression, and to compare these changes with those in the parathyroid gland in a Wistar-Hannover rat model. We hypothesized that (i) IR would induce detectable structural injury in thyroid follicles at this early time point, and (ii) HSP-90 expression patterns might diverge between thyroid and parathyroid tissues, reflecting organ-specific radiosensitivity and stress adaptation.

Materials and Methods

Experimental animals

Male Wistar-Hannover rats, six weeks old and weighing 250-350 g, were obtained from the animal laboratory of our institution. Animals were housed under specific pathogen-free (SPF) conditions with controlled temperature and humidity and a 12:12-hour light-dark cycle. Standard chow and water were provided ad libitum.

Ethical Approval

All animal procedures were reviewed and approved by the Bağcılar Training and Research Hospital Animal Experiments Local Ethics Committee (HADYEK) under approval number **HADYEK/2024-14**, decision no: **2024/49**, and were conducted in full compliance with national regulations and **ARRIVE guidelines** for the reporting of animal research.

Grouping and irradiation protocol

Eighteen rats were randomly allocated into two groups (n = 9 each): a control group and an irradiation (IR) group. Group allocation was balanced according to baseline body weight to minimize potential confounding. In the IR group, animals were anesthetized with intraperitoneal ketamine (70 mg/kg) and xylazine (7 mg/kg). Under anesthesia, rats were positioned and immobilized, and a single dose of 18 Gy was delivered to the head and neck region using a Varian Clinac iX linear accelerator. Field size and positioning were standardized to encompass the thyroid and parathyroid regions while minimizing

unnecessary whole-body exposure. Preparation and irradiation lasted approximately 30-45 minutes per animal.

Following irradiation, animals were returned to the animal facility while still anesthetized. To prevent hypothermia, recovery was conducted on a heated operating table and in an intensive care unit as needed. Rats were returned to group cages only after complete recovery from anesthesia. Control animals underwent handling and anesthesia without irradiation.

Clinical monitoring and euthanasia

Body weight was recorded at baseline and regularly monitored throughout the 21-day follow-up. The expected weight loss under the given conditions with a normal diet was ≤10-11%; supplemental nutrition was planned only if clinically indicated. On day 21 after irradiation (early post-exposure time point), all animals were euthanized by decapitation under deep anesthesia, and thyroid and parathyroid tissues were immediately harvested for pathological evaluation. To avoid unnecessary animal use, remaining carcasses were stored for subsequent research purposes in accordance with national regulations (Official Journal, 15 February 2014, Article 8, paragraph 8, letter k).

Histopathological processing

Thyroid and parathyroid tissues were carefully dissected under a stereomicroscope. Particular attention was paid to identifying parathyroid tissue based on its typical location relative to the thyroid lobes and its distinct microscopic appearance. Samples were fixed in 10% neutral buffered paraformaldehyde for 24 hours, dehydrated through graded alcohols, cleared in xylene and embedded in paraffin. Serial 4-µm sections were cut and mounted on glass slides.

Hematoxylin and eosin (H&E) staining was performed following standard protocols. Histopathological evaluation focused on follicular architecture, colloid characteristics, vascular structures and inflammatory infiltration. Congestion, inflammation and epithelial desquamation were semi-quantitatively assessed by an experienced pathologist blinded to group allocation, and scores were used for statistical comparison between groups.

Immunohistochemistry for HSP-90

For immunohistochemical analysis, paraffin sections were deparaffinized, rehydrated and subjected to heat-induced antigen retrieval. Endogenous peroxidase activity was blocked, and non-specific binding was minimized using appropriate blocking solutions. Sections were incubated with a polyclonal rabbit anti-HSP-90 antibody (Cell Signaling Technology, Massachusetts, USA), followed by a suitable secondary antibody and chromogenic detection using a peroxidase-based system. Counterstaining was performed with hematoxylin.

Cytoplasmic HSP-90 immunoreactivity in thyroid and parathyroid tissues was evaluated by light microscopy. For the purposes of this study, expression was categorized as preserved (positive

cytoplasmic staining in follicular cells or parathyroid chief cells) or lost/markedly reduced (absence or near-complete loss of specific cytoplasmic staining). Evaluation was performed by a pathologist blinded to group allocation.

Statistical analysis

Data are presented as median (minimum-maximum). Between-group comparisons (control vs IR) for histopathological scores and HSP-90 expression were conducted using the Mann-Whitney U test. A two-sided p-value < 0.05 was considered statistically significant. Statistical analyses were performed using standard statistical software. Given the exploratory nature of this animal study and the limited sample size, no formal power calculation was performed a priori; findings should therefore be interpreted as hypothesis-generating.

Results

Histopathological alterations in the thyroid gland on day 21 after irradiation, pronounced structural alterations were observed in the thyroid glands of the IR group compared with controls. Vascular congestion was significantly increased in irradiated animals ($p = 0.031$), accompanied by enhanced inflammatory cell infiltration in the interfollicular stroma ($p = 0.040$). Epithelial desquamation, reflected by partial detachment and shedding of follicular cells into the colloid or follicular lumen, was also significantly more prominent in the IR group ($p = 0.006$). Collectively, these changes indicate early post-irradiation damage at both vascular and epithelial levels (table 1) (figure 1).

In contrast, control animals showed preserved follicular architecture with regular colloid, minimal congestion and only sparse inflammatory cells (figure 2). Thyroid volume and global architecture were grossly maintained in both groups at this time point, but the qualitative differences in microstructural integrity were evident.

HSP-90 expression in the thyroid

Immunohistochemical analysis revealed a paradoxical pattern of HSP-90 expression. In the control group, thyroid follicular cells exhibited robust cytoplasmic HSP-90 staining, consistent with the high metabolic activity and basal need for chaperone support (figure 3). In the IR group, however, HSP-90 immunoreactivity in follicular cells was significantly reduced, with a higher frequency of specimens classified as loss or marked reduction of staining ($p = 0.011$) (figure 4). This indicates that, at day 21 post-irradiation, thyroid HSP-90 levels are lower in irradiated animals compared to non-irradiated controls, contrary to the classical expectation of stress-induced HSP upregulation (table 1).

Parathyroid morphology and HSP-90 expression

Parathyroid glands, identified adjacent to the thyroid lobes, did not show overt architectural disruption at this early time point. Chief cells remained arranged in cords with preserved cellular density, and no consistent pattern of marked congestion or inflammatory infiltration was detected.

Regarding HSP-90, cytoplasmic expression in parathyroid chief cells did not differ significantly between control and IR groups ($p = 0.914$). Expression was generally preserved in both groups, suggesting a more stable chaperone profile in parathyroid tissue under the given exposure conditions and within the observed time window (table 1) (figure 4).

Overall, these findings indicate that a single 18 Gy IR exposure induces clear early morphological injury and a paradoxical reduction in HSP-90 expression in the thyroid gland, whereas parathyroid glands display relative morphological and molecular stability at day 21.

Discussion

This experimental study investigated the early post-irradiation (day 21) effects of a single high-dose ionizing radiation (IR) exposure on thyroid and parathyroid tissues, focusing on histopathological integrity and HSP-90 expression. The findings demonstrate that IR induces significant vascular and epithelial injury in the thyroid gland, accompanied by a paradoxical reduction in HSP-90 expression, whereas the parathyroid gland exhibits relative structural and molecular stability at this early time point. The observed increases in vascular congestion, inflammatory infiltration, and epithelial desquamation are consistent with the known radiosensitivity of thyroid tissue and likely reflect endothelial damage, microcirculatory disturbance, and oxidative stress-mediated cellular injury [20,22,23]. These early microstructural alterations may constitute the histological substrate for later functional impairment, including hypothyroidism and nodular disease [10-13,22,23]. The most notable finding of this study is the paradoxical downregulation of HSP-90 in thyroid follicular cells, which contrasts with the classical view of HSP-90 as a stress-inducible chaperone that is typically upregulated under proteotoxic conditions [17-19,23]. A mechanistically plausible explanation for this observation is a temporal biphasic response pattern in the cellular stress machinery following ionizing radiation. In the early post-irradiation phase, acute DNA damage, mitochondrial dysfunction, and ATP depletion may induce a global suppression of protein synthesis, including stress-inducible chaperones such as HSP-90, reflecting a transient energy-conserving state in highly metabolically active thyroid follicular cells [20,21]. As cellular recovery mechanisms are progressively engaged, a delayed compensatory upregulation of HSP-90 and related chaperones may occur at later time points, restoring proteostasis and supporting cellular adaptation [20,21]. This biphasic trajectory may reconcile the apparent discrepancy between our findings and studies reporting increased HSP expression under chronic or prolonged stress conditions [16,20,21,23]. Additional mechanisms may further contribute to this paradoxical response, including inhibition of ribosomal RNA synthesis, nucleolar dysfunction, and altered thyroid hormone signaling pathways affecting HSP-90 regulation [18,19,24].

In contrast, the relative preservation of parathyroid morphology and stable HSP-90 expression suggest that structural organization and metabolic demand may underlie organ-specific differences in radiosensitivity; the absence of follicular architecture and comparatively lower synthetic activity in parathyroid tissue may confer resilience against early proteostatic disruption [11,16]. Nevertheless, alternative explanations, including distinct temporal dynamics of stress responses in parathyroid cells,

cannot be excluded [11,16]. Several limitations should be acknowledged, including the use of a single time point, the relatively small sample size, and the semi-quantitative assessment of HSP-90 expression.

Furthermore, the use of a single high radiation dose does not fully replicate fractionated clinical regimens, and the absence of additional proteostasis markers limits broader mechanistic interpretation. Future studies incorporating multiple time points, quantitative approaches, and expanded evaluation of the chaperone network, together with functional endocrine assessments, are warranted to clarify the temporal dynamics and mechanistic basis of radiation-induced endocrine injury.

Future directions

Future studies should address these limitations by incorporating multiple time points, different total doses and fractionation schemes, and more comprehensive evaluation of the chaperone network. Integration of hormonal measurements (TSH, T3, T4, PTH) and functional endpoints would allow correlation of structural and molecular alterations with endocrine outcomes. Intervention studies using antioxidants, radioprotective agents or pharmacological inducers of HSP-90 could clarify whether modulation of proteostasis can mitigate IR-induced thyroid injury. Finally, systems-level approaches (proteomics, transcriptomics) targeting HSP-90-associated signaling pathways (e.g., PI3K/Akt, MAPK, p53) may provide deeper mechanistic insight into how IR reshapes the cellular stress landscape in endocrine tissues.

Conclusion

In summary, this experimental study demonstrates that a single high-dose IR exposure to the head and neck region induces early microstructural injury in the rat thyroid, characterized by increased vascular congestion, inflammatory infiltration and epithelial desquamation, while paradoxically reducing HSP-90 expression in follicular cells at day 21. In contrast, parathyroid glands display relative morphological and molecular stability under the same conditions. These findings refine our understanding of organ-specific radiosensitivity within the endocrine system and suggest that early suppression of HSP-90-mediated proteostasis may be a key component of radiation-induced thyroid vulnerability. Elucidating the temporal and mechanistic details of this response may open avenues for targeted radioprotective strategies and improved management of thyroid dysfunction in patients undergoing head and neck irradiation.

Declarations

Funding

This research received no specific grant from any funding agency in the public, commercial, or not-for-profit sectors.

Conflicts of Interest

The authors declare that they have no conflicts of interest.

Ethics Approval

All experimental procedures involving animals were reviewed and approved by the Bağcılar Training and Research Hospital Animal Experiments Local Ethics Committee (HADYEK), under approval number **HADYEK/2024-14**, decision no **2024/49**. All procedures complied with institutional guidelines, national regulations, and **ARRIVE** reporting standards.

Consent to Participate

Not applicable.

Consent for Publication

Not applicable.

Availability of Data and Materials

The datasets generated and analyzed during the current study are available from the corresponding author on reasonable request.

Authors' Contributions

All authors contributed to the study conception, experimental design, data acquisition, analysis, and manuscript preparation. All authors read and approved the final manuscript.

Acknowledgements

None.

References

1. Hall EJ, Giaccia AJ (2018) Radiobiology for the radiologist. 8th ed. Philadelphia: Lippincott Williams & Wilkins
2. Furukawa K, Preston DL, Funamoto S et al. (2013) Long-term trend of thyroid cancer risk among Japanese atomic-bomb survivors: 60 years after exposure. Int J Cancer 132(5):1222–1226. **doi: 10.1002/ijc.27749**
3. Podgorsak EB (2010) Radiation physics for medical physicists. 2nd ed. Berlin / Heidelberg: Springer
4. ICNIRP (International Commission on Non-Ionizing Radiation Protection) (2020) ICNIRP statement: principles for non-ionizing radiation protection. Health Phys.;118(5):477–482. doi:10.1097/HP.0000000000001252
5. Saenko V, Thomas GA, Suzuki H et al. (2024) Radiation-related thyroid cancer: biological mechanisms and clinical implications. Endocr Rev 45(1):1–52. doi:10.1210/endrev/bnad032.

6. Joiner MC, van der Kogel AJ (Eds) (2018) Basic clinical radiobiology. 5th ed. Boca Raton: CRC Press doi:10.1201/9780429490606
7. Iglesias ML, Schmidt A, Al Ghuzlan A et al. (2017) Radiation exposure and thyroid cancer: a review. Arch Endocrinol Metab 61(2):180–187. doi:10.1590/2359-3997000000257
8. Anderson G, Ebadi M, Vo K et al. (2021) An updated review on head and neck cancer treatment with radiation therapy. Cancers (Basel) 13(19):4912. doi:10.3390/cancers13194912.
9. Teimouri K, Pakravan S, Rahmatinia E et al. (2022) Evaluation of radiation side effects on thyroid function. J Parathyr Dis 10:e9145. doi:10.34172/jpd.2022.9145
10. Drozdovitch V, Bouville A. (2021) Radiation exposure to the thyroid after the Chernobyl accident. Front Endocrinol (Lausanne) 12:699171. doi:10.3389/fendo.2021.699171
11. Iványi G, Christofi A, Sipka G et al. (2025) Radiation-induced synchronous parathyroid carcinoma and papillary thyroid carcinoma: clinical, morphological, and genetic insights. Int J Mol Sci 26(9):4441. doi:10.3390/ijms26094441
12. Colaprico C, Lomartire F, Raccio Iet al. (2025) Low-dose ionizing radiation and thyroid diseases and functional modifications in exposed workers: a systematic review. J Clin Med 14(2):588. doi:10.3390/jcm14020588
13. Nikiforov YE. (2006) Radiation-induced thyroid cancer: what we have learned from Chernobyl. Endocr Pathol 17(4):307–318. doi:10.1007/s12022-006-0001-5.
14. Hall JE, Hall ME. (2020) Guyton and Hall textbook of medical physiology. 14th ed. Philadelphia: Elsevier
15. Spitz DR, Azzam EI, Li JJ et al. (2004) Metabolic oxidation/reduction reactions and cellular responses to ionizing radiation: a unifying concept in stress response biology. Cancer Metastasis Rev. 23(3–4):311–322. doi:10.1023/B:CANC.0000031769.75846.64
16. Misa-Agustíño MJ, Jorge-Mora T, Jorge-Barreiro FJ et al. (2015) Exposure to non-ionizing radiation provokes changes in rat thyroid morphology and expression of HSP-90. Exp Biol Med (Maywood). 240(9):1123–1135. doi:10.1177/1535370214567611
17. Maiti S. (2022) Cytosolic Hsp90 isoform-specific functions and clinical implications. Trends Cell Biol. 32(10):841–855. doi:10.1016/j.tcb.2022.08.002
18. Pratt WB, Toft DO. (2003) Regulation of signaling protein function and trafficking by the HSP90/HSP70-based chaperone machinery. Exp Biol Med (Maywood). 228(2):111–133. doi:10.1177/153537020322800201
19. Fan L, Kishore A, Jansen-Olliges L et al. (2022) Identification of a thyroid hormone binding site in Hsp90 with implications for its interaction with thyroid hormone receptor beta. ACS Omega. 7(33):28932–28945. doi:10.1021/acsomega.2c02331
20. Valko M, Leibfritz D, Moncol J et al. (2007) Free radicals and antioxidants in normal physiological functions and human disease. Int J Biochem Cell Biol. 39(1):44–84. doi:10.1016/j.biocel.2006.07.001

21. **Misa-Agustiño MJ, Leiro JM, Jorge-Mora MT et al. (2012) Electromagnetic fields at 2.45 GHz trigger changes in heat shock proteins 90 and 70 without altering apoptotic activity in rat thyroid gland. Biol Open. 1(9):831–838. doi:10.1242/bio.20121297.**
22. Indrasari SR, Solikin N, van Diessen NA et al. (2024) Radiation-induced thyroid gland changes in nasopharyngeal carcinoma patients after chemoradiotherapy. Asian Pac J Cancer Care. 9(4):667–672. doi:10.31557/apjcc.2024.9.4.667-672
23. Soudry E, Stern Shavit S, Hardy B et al. (2017) Heat shock proteins HSP90, HSP70 and GRP78 in medullary thyroid carcinoma. Thyroid Res. 10:9. doi:10.1186/s13044-016-0039-8
24. Fan L, Kishore A, Jansen-Olliges L et al. (2022) Identification of a thyroid hormone binding site in Hsp90 with implications for its interaction with thyroid hormone receptor beta. ACS Omega. 7(33):28932–28945. doi:10.1021/acsomega.2c02331

Table

Table 1. Histopathological and Immunohistochemical Findings in Control and Irradiated Groups

Variable	Control Group (Median, min-max)	Irradiated Group (Median, min-max)	p-value (Mann-Whitney U)
Congestion	1 (0-1)	1.5 (1-2)	0.031
Inflammation	0 (0-0)	1 (0-2)	0.040
Epithelial desquamation	0 (0-0)	1.5 (1-2)	0.006
HSP-90 (thyroid)	2 (2-3)	1 (1-2)	0.011
HSP-90 (parathyroid)	2.5 (2-3)	2.5 (1-3)	0.914

Figures

Figure 1:

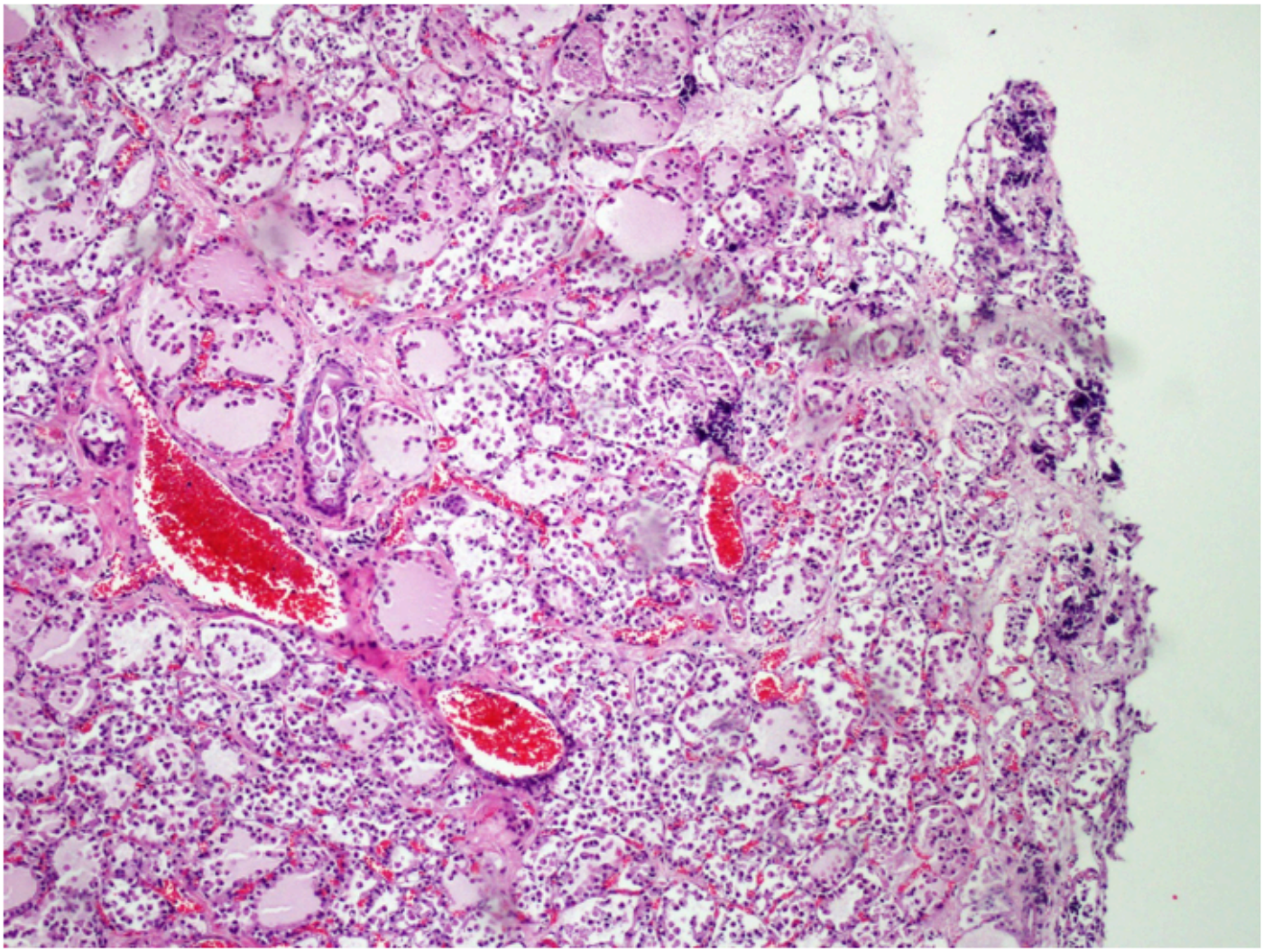


Figure 1

Following exposure to ionizing radiation, thyroid tissue exhibits marked epithelial desquamation in follicular structures, vascular congestion, and inflammatory infiltration (H&E, 200×).

Figure 2:

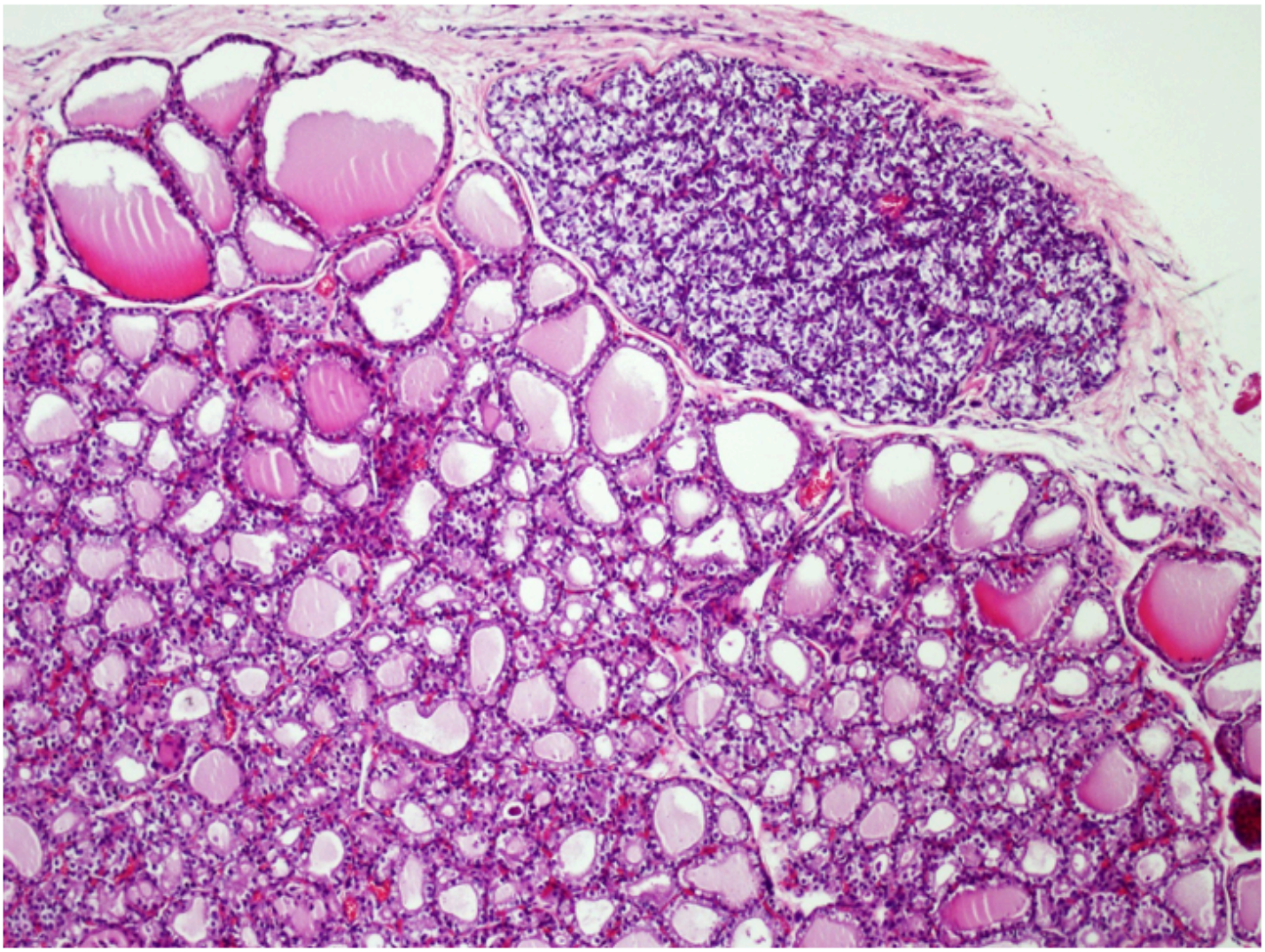


Figure 2

Vascular and follicular structures, as well as parathyroid tissue, appear within normal histological limits in control thyroid tissue not exposed to ionizing radiation (H&E, 200×).

Figure 3:

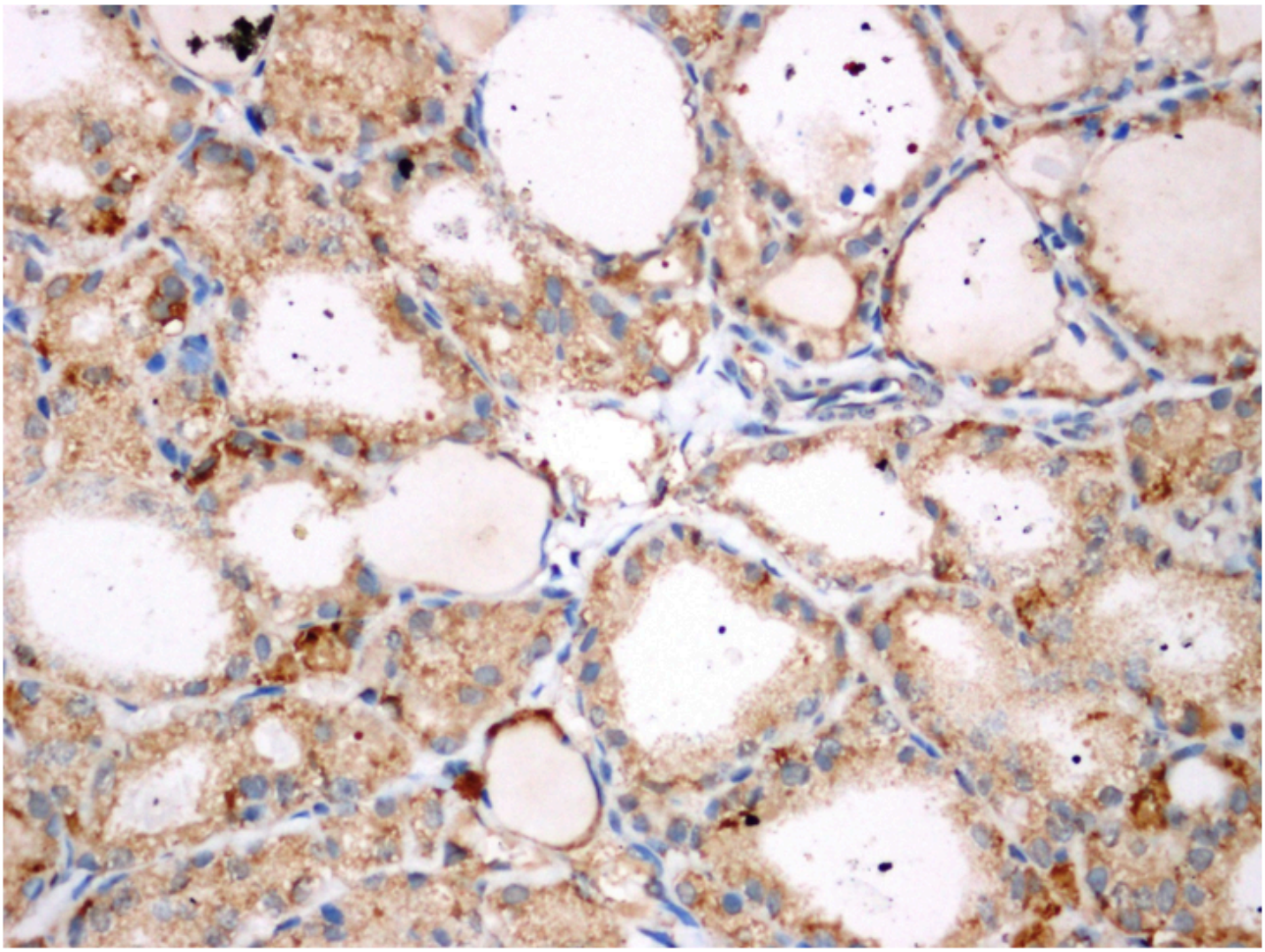


Figure 3

Strong cytoplasmic HSP90 expression is evident in control thyroid tissue (IHC, anti-HSP90, 400×).

Figure 4:

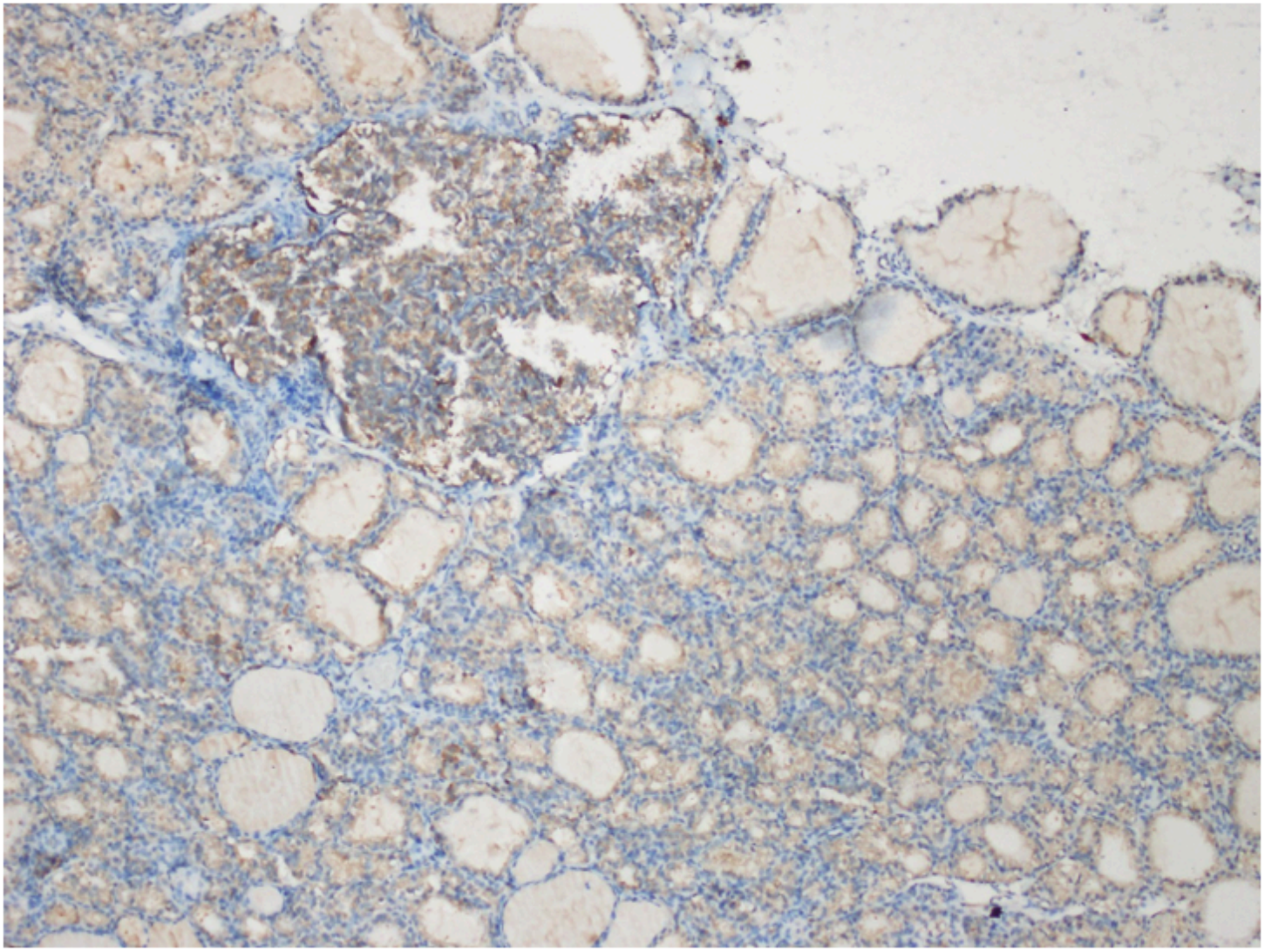


Figure 4

After ionizing radiation exposure, HSP90 expression is markedly reduced in thyroid tissue, whereas cytoplasmic HSP90 expression persists in parathyroid tissue (IHC, anti-HSP90, 200×).

Supplementary Files

This is a list of supplementary files associated with this preprint. Click to download.

- Table1.docx